

## EHEHP DATABASE TO PREDICT RARE EARTH SOLVENT EXTRACTION

By

Leslie Miller and AJ Gerbino

OLI Systems, Inc, USA

Corresponding Author

Anthony Gerbino

Aj.gerbino@olisystems.com

Presenter

Leslie Miller

leslie.miller@olisystems.com

### ABSTRACT

We combined a semi-empirical extractant database, a rigorous electrolyte thermodynamic model, and a process simulator to predict solvent extraction of rare earth elements from an  $\text{HNO}_3$  solution to a hydrocarbon phase. We then predicted the extractant regeneration and metals separation using a caustic solution.

We created the extractant database using publicly available data for HEHEHP and its reactivity with fifteen rare earth elements. The data included extractant solubility in water, metal extraction isotherms, distribution ratios, dimerization constants, acidity constants and heats of saponification. We created several species for each extractant including the base acid, the ionized acid, and the dimerized acid. We also created several metal-extractant complexes for each of the rare earth elements. In total, over 100 individual species were created for the fifteen rare earth metals with the extractant.

We combined the database with an electrolyte thermodynamic model to compute the liquid-liquid partitioning of the following systems:  $\text{H}_2\text{O}$ -extractant,  $\text{H}_2\text{O}$ -extractant-diluent, and  $\text{H}_2\text{O}$ - $\text{HNO}_3$ - $\text{RE}(\text{NO}_3)_3$ -extractant-diluent. We can match with reasonable accuracy the extractant solubility in water, the heats of saponification, and the partitioning isotherms for all fifteen rare earth elements. We also predicted with limited accuracy, the effects of pH, diluent:extractant ratio, total ion concentration, and temperature on metal partitioning. We present the partitioning isotherms for each element in the individual extractant/diluent mixtures and when both extractants are in a 50:50 mixture.

We then used the speciation model with a process simulator to calculate the mass, chemistry, and energy balance across a series of solvent extraction units. We simulated the process without and with mass transfer limiting parameters. We obtained a reasonable match between predicted and reported extraction efficiencies when we include mass-transfer parameters.

Lastly, we identified areas where we can improve existing chemical properties and partitioning mechanisms and where additional experimental data is needed to make a model more robust.

*Keywords: Rare Earth, Solvent Extraction, process simulation*

### INTRODUCTION

Solvent extraction is an industry-accepted method for separating rare earth elements from pregnant liquor. A commonly-used extractant is HEHEHP, which is identified in the literature by its product identification P-507 or PC88A (HEHEHP) or by its trade name, Isonquest 801 (Italmach Chemicals AWS®). There are research papers available that report the performance of this chemical for extracting dissolved rare earth metals from nitric and hydrochloric acid solutions. Our goal was to process the extraction data from these papers and create a speciation-based predictive model with the fifteen rare earth elements in  $\text{HNO}_3$ . The outcome is the ability to model solvent extraction using engineering software to design and optimize solvent extraction operations.

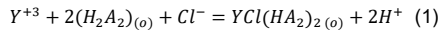
This paper reports on the quantitative study performed in this area. Literature data and plots were used to back calculate the following:

- The extraction isotherms as extractant concentration varies,
- The extraction efficiency as pH varies,
- The coordination chemistry of rare earths with the extractant and  $\text{NO}_3^{-1}$  and as pH and concentration change,
- The solubility and partitioning of extractants with water and hydrocarbon, and
- The enthalpies for each of the reactions.

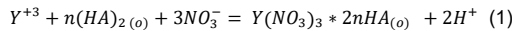
Our study focuses on the chemistry of extraction and not the engineering. In this way, the predictions can be used across multiple engineering platforms. Although there are many papers written on extractants, we had limited success finding thermodynamic data (G, H, S, Cp, V). We therefore estimated these values by curve fitting available plots reported or other disparate data points. Consequently, the current predictions are estimations that can be improved once additional scientific data becomes available.

### LITERATURE DATA

We searched for literature data containing information on some or all of the following components: HEHEHP, rare earth elements,  $\text{HNO}_3$ , and hydrocarbon (decane, kerosene, toluene, etc.). We found information on chemical speciation, distribution ratios, separation factors, pKa's plus other equilibrium constants, and partitioning isotherms. Zhang for example studied yttrium extraction using HEHEHP and Cyanex 272 from chloride solutions. They reported HEHEHP separation factors,  ${}^{11}\beta_{(Z+1/Z)} = 3.04$  and 1.60 with extraction equilibrium equation as follows,



A is the HEHEHP molecule and  $H_2A_2$  is its dimerized form in the immiscible phase. The author also provided plots which were used to curve fit the thermodynamic partitioning coefficients. Qi provides several important plots and a table containing equilibrium constants, distribution ratios, separation factors of adjacent rare earth elements and changes in G, H, and S following extraction. Although these data cannot be used directly (they are measurements) they can be used to confirm the properties created for each of the reacting and product species entered in the database. Qi also identified the following reaction as the main solvation extraction reaction. <sup>ii</sup>

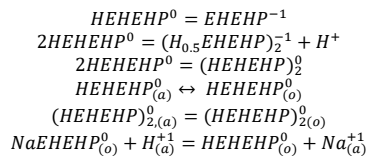


The coefficient  $n$  is the solvation number of HA for the reaction. Many of the plots and data provided in the Qi text are presented in journal articles by this author and others. So, this book is a good compilation for the data we needed to complete the effort.

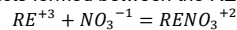
Zhao et al provided useful plots on La and Ce extraction with HEHEHP as a function of extractant concentration and pH. These plots are used in the current work. Mohammadi et al., studied ND, Dy, and Y separation from HCl solutions using HEHEHP and D2EHP. They reported equilibrium constants, chemical reactions, distribution ratios, separation factors, and isotherm plots. This was a key reference paper for developing our predictions. <sup>iiiiv</sup>

### APPROACH

We used OLI software (OLI Systems, Inc)<sup>2</sup> to complete this work. We created a custom database containing three sets of species. The first set is for HEHEHP speciation with water and NaOH. This includes acid ionization, dimerization, and partitioning to the immiscible phase.



The second set included reaction products formed between the  $\text{REY}^3$  and  $\text{HNO}_3^4$



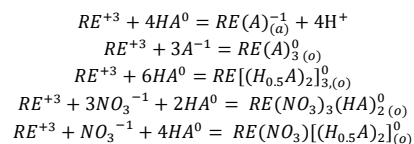
<sup>1</sup> Rhodia Technical bulletin.

<sup>2</sup> OLI Software tools used include OLI StreamAnalyzer, OLI Databook, and OLI Flowsheet+Optimizer.

<sup>3</sup> REY=rare earth elements and yttrium

<sup>4</sup> Pm is not included.

The final set of species were the reactions products between REY and the extractants.



There is limited x-y (tabular) data provided in the literature. There are however several plots containing isotherms, distribution ratios, and separation factors. We then fit our predictions to this and other data.

### CURVE FITTING RESULTS

#### HEHEHP + HNO<sub>3</sub>

Figure 1 is a comparison plot for the fifteen rare earth elements. The thick black lines and circles are results reported by Qi (2018). The thin, colored lines are the current predictions. The conditions are 0.03 m RE and 1 m HEHEHP. Starting HNO<sub>3</sub> concentrations range from 0.9 to 1.5 m and NaOH is added to adjust pH. To go to lower pH's (higher lg[H<sup>+</sup>] values), HNO<sub>3</sub> is added beyond the starting amounts.

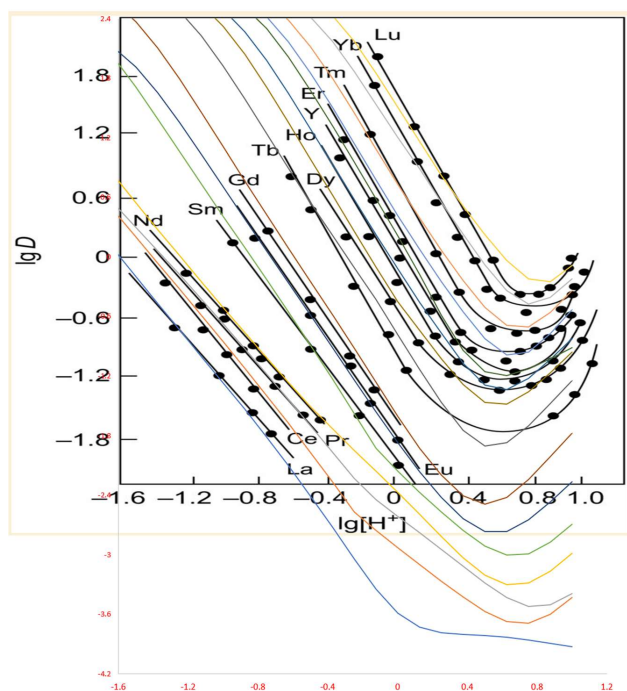
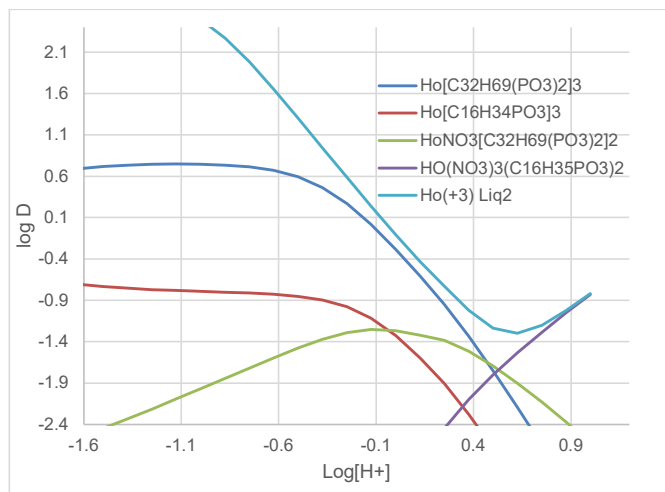


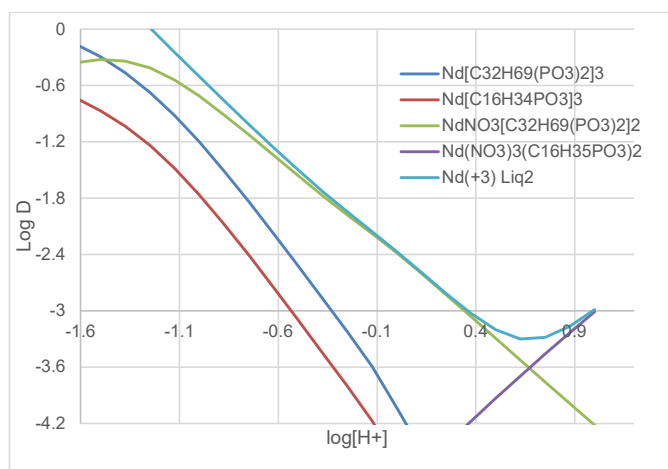
Figure 1 - Comparison between predictions and measured distribution ratios. Plot extracted from Dezhi Qi. 2018.

The predictions show good fit with the slope of each element and the impact of HNO<sub>3</sub> (pH) on the partitioning matches where the curve increases. The effects of NO<sub>3</sub><sup>-1</sup> on Ho partitioning are shown in Figure Figure 2. At high pH, the dominant complex is Ho[H(EHEHP)<sub>2</sub>]<sub>3</sub>. At high HNO<sub>3</sub> concentrations, lower pH, the two NO<sub>3</sub>-containing complexes become important and cause the distribution ratio to increase.



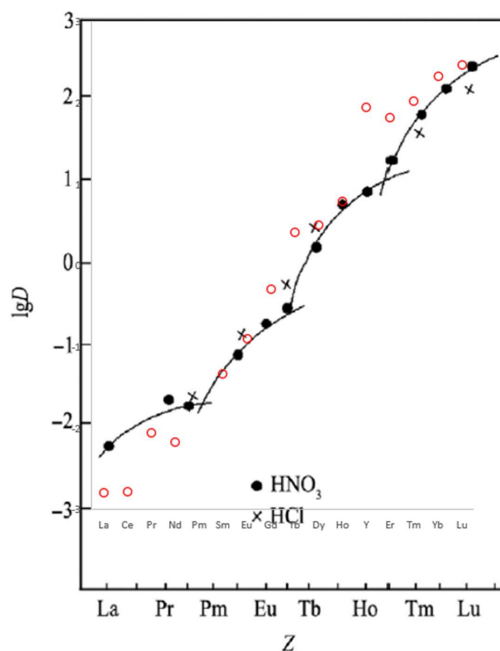
**Figure 2 - Contribution of four Re-NO<sub>3</sub>-HEHEHP complexes to the overall Ho distribution ratio**

By comparison, Nd speciation (Figure 3) required that dominant complex be  $\text{Nd}(\text{NO}_3)(\text{HA}_2)_2$  in order to match the isotherm plot in Figure 1 but to still show similar curvature as the other elements. This included the slope of the isotherm. Similar speciation was used to match the curves for La, Ce, and Pr. We still are unsure what contribution the  $\text{Re}[\text{HEHEHP}]_3$  complex has. This complex is reported in the literature, but it does not seem to be needed. Also, since the HEHEHP dimerizes in the non-aqueous phase, this complex is not important to modelling RE partitioning.



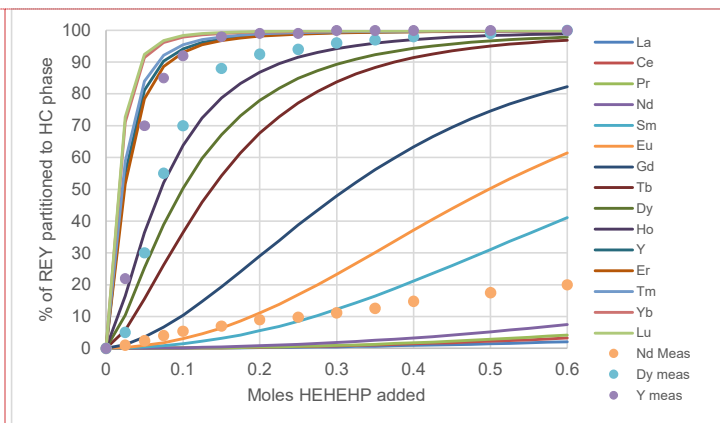
**Figure 3 - Contribution of four RE-NO<sub>3</sub>-HEHEHP complexes to the overall Nd distribution ratio**

Figure 4 is a comparison plot between the predicted Log D values and those reported by Qi (2018). We could not find the precise composition for this published plot and therefore used 0.005 m RE, 0.15 M HEHEHP, 0.132 m  $\text{HNO}_3$  (pH=1) and 1L n-C13. There is good qualitative fit for most, but not for the four LREE and for Y. We think that this can be improved by modifying the  $\text{RE}(\text{NO}_3)(\text{H}[\text{EHHP}]_2)_2$  and  $\text{RE}(\text{NO}_3)_3(\text{H}[\text{EHHP}]_2)$  stability constants but would need more precise data to support this.



**Figure 4 - Distribution ratio comparison for each RE. The open red circles are the predictions. The black lines, closed circles, and x's are the reported values.**

Figure 5 is a plot of the partitioning isotherms for the fifteen REY as a function HEHEHP addition. Conditions were 0.01 mole of each rare earth element, 0.132 m HNO<sub>3</sub>, 1 L of tridecane, and 0 to 0.6 moles HEHEHP. Also plotted are Nd, Dy, and Y isotherm data reported by Mohammadi et al for same set of experiments but when using HCl<sup>19</sup>. The plot shows the similar groupings of elements shown in Figure 4 and as reported in the literature. The lowest grouping La, Ce, Pr, and Nd have weaker isotherms than reported for Nd with HCl, and although this is a different complex with different stabilities, the weaker isotherms are consistent with the lower than reported LogD shown in Figure 4. This is the result the slope and curve match work shown in Figure 1. The isotherms for Dy and Y are similar to Mohammadi et al, and this is also consistent with Figure 2 where we calculated that the dominant complex is the RE(HA<sub>2</sub>)<sub>3</sub>, a complex that is independent of the electrolyte used.



**Figure 5 – Plot of the calculated isotherms for the fifteen rare earth metals.**

**Commented [LM1]:** @AJ Gerbino please add Description to Figure 5 and add text to reference Figure 5. I will review and then we should be ready to submit.

## APPLYING THE PREDICTIONS

Figure 6 is an image of a simulated solvent extraction process that separate Lu, Y, Gd, Eu, Nd, and La. It contains twenty-three separation stages divided into four sections. The first four stages (section #1) remove Lu, the next seven stages (section #2) remove Y, the next eight stages (section #3) remove Gd and Eu, and the final four stages (section #4) separates Nd from La. Each stage is modelled isothermally at 20 C. Phase separation (electrolyte from solvent) is complete – we did not simulate entrainment/inefficient separation effects. The loaded electrolyte stream flows through all twenty-three units. Fresh extractant is added in each separation section.

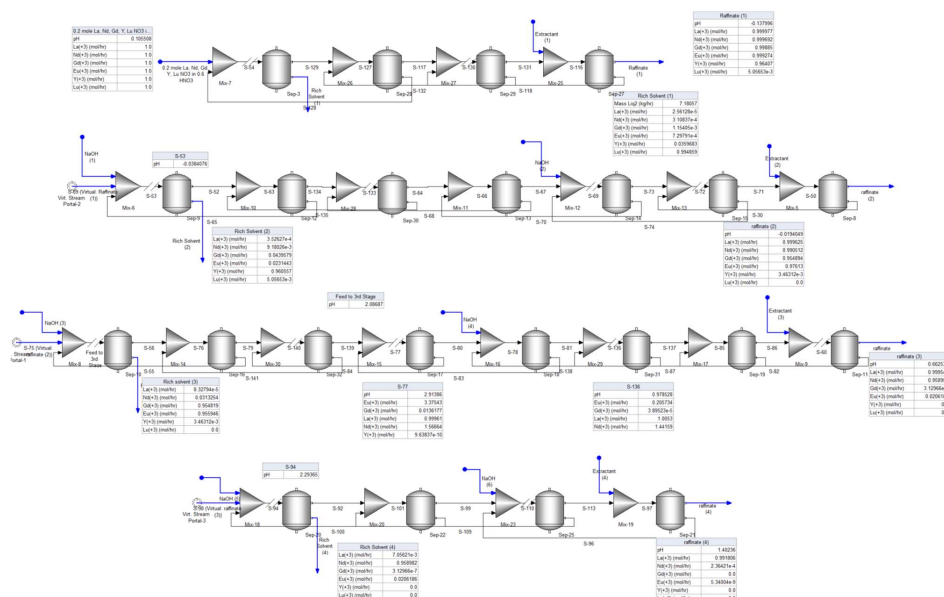


Figure 6 – Simulating four-step extraction of six rare-earth elements

The loaded electrolyte flows into the process at 8 kg/hr (6.2 L/hr). It contains 1 mole each of  $\text{Lu}(\text{NO}_3)_3$ ,  $\text{Y}(\text{NO}_3)_3$ ,  $\text{Gd}(\text{NO}_3)_3$ ,  $\text{Eu}(\text{NO}_3)_3$ ,  $\text{Nd}(\text{NO}_3)_3$ , and  $\text{La}(\text{NO}_3)_3$ , 4 moles of  $\text{HNO}_3$ , and 320 moles (5765.8 g) of  $\text{H}_2\text{O}$ . The electrolyte pH is 0.1 and the feed temperature is 20 C. The extractant (HEHEHP+diluent) composition is 19.6 mol% HEHEHP, 21.6 mol% n-C<sub>10</sub>, 39.2 mol% n-C<sub>13</sub>, and 19.6 mol% n-C<sub>16</sub>. The extractant flows into the process at four locations, one for each separation section. It flows at 7, 21, 6.4, and 4 kg/hr for Sections 1, 2, 3, and 4, respectively. That is 39.4 kg/hr solvent for 8 kg/hr electrolyte or 36.3 moles of HEHEHP per 6 moles of rare earths (6:1 mole ratio).

The caustic stream is 10 m NaOH and enters at six locations, none in section #1, twice in section #2, twice in section #3 and twice in section #4. A total of 1.83 kg/hr (45.75 mole) NaOH is added. We fixed the caustic feed in sections #2 and #4 to reach an average pH of ~0 and ~1.7, respectively. We used an equation-based tool to find the optimal extraction pH in section #3. The optimization objective was defined to maximize Gd and Eu removal while minimizing Nd loss. The optimal pH in Section #3 was between 0.9 and 1.5, depending on the stage.

We then performed a caustic feed sensitivity study in section #3 to test the pH effects on Gd, Eu, and Nd removal efficiency. Lastly, we varied section #3 stages between 5 and 15 while optimizing caustic addition to separate Gd from Eu.

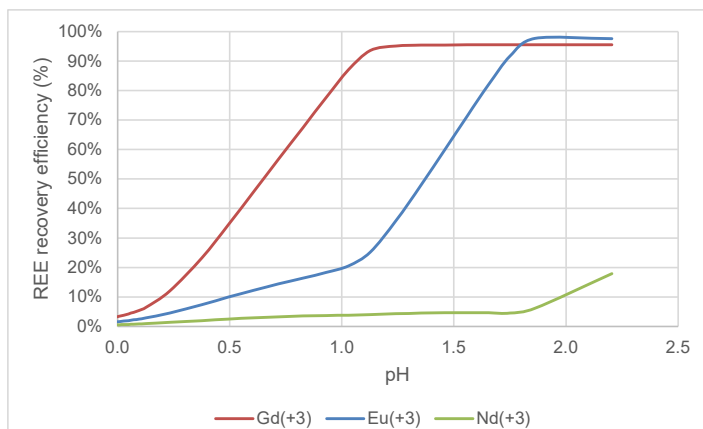
## Results

Table 1 contains the simulation results for the rich solvent stream exiting the process after optimizing the caustic feed to section #3. Each column represents the rare earth metal recovery after each section. The first column shows that 99.5% of Lu that enters the process is recovered in this section #1. Also, 3.6% of the Y and 0.12% of Gd is removed. Section #2 removes 96.1% of the added Y into the rich solvent. This solvent is also computed to extract 4.4% of Gd and 2.3% of Eu. It is very likely that with additional separation stages (eight are used in this section) a purer Y-rich solvent would be computed.

**Table 1 - Element recovery in the rich solvent following each separation section.**

Element	Section #1	Section #2	Section #3	Section #4
La(+3)	0.00%	0.04%	0.01%	0.71%
Nd(+3)	0.03%	0.92%	3.13%	95.90%
Eu(+3)	0.07%	2.31%	95.59%	2.06%
Gd(+3)	0.12%	4.40%	95.48%	0.00%
Y(+3)	3.60%	96.06%	0.35%	0.00%
Lu(+3)	99.49%	0.51%	0.00%	0.00%

Figure 7 is a plot showing the effects of section #3 raffinate pH on the Gd and Eu extraction efficiency. The section #3 raffinate pH is on the lower end of the pH value across the eight stages. Above 1.2 pH, about 90+% of Gd is recovered. Above 1.7 pH, both Gd and Eu are recovered at 95+%. Also, above 1.7 pH, Nd extraction starts to increase, which limits the optimal separation range.



**Figure 7 - Optimizing Gd/Eu separation from Nd using pH control.**

Figure 8 is a plot of the Eu-Gd separation efficiency as the number of stages in Section #3 varies from 5 to 15. The caustic and extractant flow rates were optimized in a similar way described above, except that Gd is maximized in the loaded solvent and Eu is maximized in the raffinate. There is a sufficient gap between the Gd and Eu isotherms in Figure 7 that would indicate by adding more stages we can separate them. By optimizing the caustic and extractant flow rates and by increasing the number of separation stages, we were able to achieve a 4.5:1 ratio of Gd:Eu in the rich solvent. This effect is already known to the industry, and so the predictions are not new. Rather, we wanted to confirm that the speciation model could predict these observations. These results also indicate a diminishing separation performance with more stages.

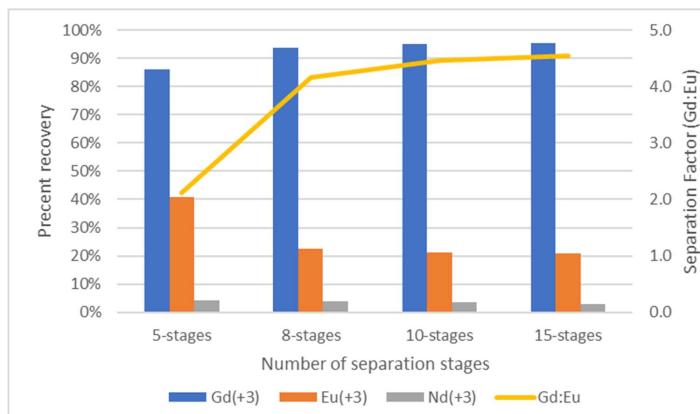


Figure 8 - Separation of Gd, Eu, and Nd as the number of separation stages vary.

### SUMMARY/CONCLUSIONS

We developed a thermodynamic database of HEHEHP and its speciation with fifteen rare earth elements. We used available literature data to derive the various complexes and their partitioning between the aqueous and organic phases. We attempted to match literature data using as few interactions and species as possible. We needed a minimum of four HEHEHP-RE complexes to match the isotherms for all fifteen elements and to match the curvature shown in Figure 1. The mole ratio of HEHEHP:RE:NO<sub>3</sub> in these complexes were 6:0:1, 3:0:1, 4:1:1 and 2:3:1. At least two are consistent with reported stoichiometries and two are inconsistent or mentioned as possible complexes.

When we used this database in a hypothetical separation process that used twenty-three separation stages. The results matched qualitatively and perhaps quantitatively the partitioning reported in the literature and the pH impact on separation. In all, the simulation achieved its intended purpose of testing the HEHEHP speciation database in a process simulation that is separating multiple elements.

<sup>i</sup> Zhang, Can, L. Wang, X. Huang, J. Donga, Z Long, and Y Zhang. 2014. Yttrium extraction from chloride solution with a synergistic system of 2-ethylhexyl phosphonic acid mono-(2-ethylhexyl) ester and bis(2,4,4-trimethylpentyl) phosphinic acid. *Hydrometallurgy*, 147–148, pp.7–12.

<sup>ii</sup> Dezhi Qi. 2018. *Hydrometallurgy of rare earths: extraction and separation*. Elsevier, Chapter 2.

<sup>iii</sup> Zhao, Z., Z.QiuJ. Yang, S. Lu, L. Cao,W. Zhang, and Y. Coin. 2017. Recovery of rare earth elements from spent fluid catalytic cracking catalysts using leaching and solvent extraction techniques. *Hydrometallurgy* 167, pp. 183–188.

<sup>iv</sup> Mohammadi, M., K. Forsberg, L. Kloo, J. Martinez De La Cruz, and Å. Rasmuson. 2015. Separation of ND(III), DY(III) and Y(III) by solvent extraction using D2EHPA and EHEHPA. *Hydrometallurgy* 156, 215–224.

<sup>v</sup> Mohammadi, M., K. Forsberg, L. Kloo, J. Martinez De La Cruz, and Å. Rasmuson. 2015. Separation of ND(III), DY(III) and Y(III) by solvent extraction using D2EHPA and EHEHPA. *Hydrometallurgy* 156, 215–224.